BJP BRITISH JOURNAL OF PHARMACOLOGY

BPS BRITISH PHARMACOLOGICAL SOCIETY

British Journal of Pharmacology (2009), 158, 339–353

0007-1188/09
www.brjpharmacol.org

THEMED ISSUE: GPCR

RESEARCH PAPER

Characterization of P2Y receptor subtypes functionally expressed on neonatal rat cardiac myofibroblasts

Amarnath Talasila, Renée Germack and John M Dickenson

Biomedical Research Centre, School of Science and Technology, Nottingham Trent University, Nottingham, UK

Background and purpose: Little is known about P2Y receptors in cardiac fibroblasts, which represent the predominant cell type in the heart and differentiate into myofibroblasts under certain conditions. Therefore, we have characterized the phenotype of the cells and the different P2Y receptors at the expression and functional levels in neonatal rat non-cardiomyocytes.
Experimental approach: Non-cardiomyocyte phenotype was determined by confocal microscopy by using discoidin domain receptor 2, α-actin and desmin antibodies. P2Y receptor expression was investigated by reverse transcription-polymerase chain reaction and immunocytochemistry, and receptor function by cAMP and inositol phosphate (IP) accumulation induced by adenine or uracil nucleotides in the presence or absence of selective antagonists of $P2Y_1$ (MRS 2179, 2-deoxy-N^6-methyl adenosine 3′,5′-diphosphate diammonium salt), $P2Y_6$ (MRS 2578) and $P2Y_{11}$ (NF 157, 8,8′-[carbonylbis[imino-3,1-phenylenecarbonylimino(4-fluoro-3,1-phenylene)carbonylimino]]bis-1,3,5-naphthalene trisulphonic acid hexasodium salt) receptors. $G_{i/o}$ and $G_{q/11}$ pathways were evaluated by using *Pertussis* toxin and YM-254890 respectively.
Key results: The cells (>95%) were α-actin and discoidin domain receptor 2-positive and desmin-negative. $P2Y_1$, $P2Y_2$, $P2Y_4$, $P2Y_6$ were detected by reverse transcription-polymerase chain reaction and immunocytochemistry, and $P2Y_{11}$-like receptors at protein level. All di- or tri-phosphate nucleotides stimulated IP production in an YM-254890-sensitive manner. AMP, ADPβS, ATP and ATPγS increased cAMP accumulation, whereas UDP and UTP inhibited cAMP response, which was abolished by *Pertussis* toxin. MRS 2179 and NF 157 inhibited ADPβS-induced IP production. MRS 2578 blocked UDP- and UTP-mediated IP responses.
Conclusion and implications: $P2Y_1$-, $P2Y_2$-, $P2Y_4$-, $P2Y_6$-, $P2Y_{11}$-like receptors were co-expressed and induced function through $G_{q/11}$ protein coupling in myofibroblasts. Furthermore, $P2Y_2$ and $P2Y_4$ receptor subtypes were also coupled to $G_{i/o}$. The G_s response to adenine nucleotides suggests a possible expression of a new P2Y receptor subtype.
British Journal of Pharmacology (2009) **158,** 339–353; doi:10.1111/j.1476-5381.2009.00172.x; published online 5 May 2009

This article is part of a themed issue on GPCR. To view this issue visit http://www3.interscience.wiley.com/journal/121548564/issueyear?year=2009

Keywords: P2Y receptors; $P2Y_{11}$-like receptors; cardiac myofibroblasts; $G_{q/11}$ and $G_{i/o}$ proteins; adenine and uracil nucleotides; YM-254890; MRS 2179; MRS 2578; NF 157; cAMP and inositol phosphate accumulation; DDR2

Abbreviations: 2-MeSADP, 2(methylthio) adenosine 5′-diphosphate; 2-MeSATP, 2(methylthio) adenosine triphosphate; ADPβS, adenosine 5′-[β-thio]diphosphate; AR-C69931MX, N6-(2-methylthioethyl)-2-(3,3,3-trifluoro-propylthio)-β, γ-dichloromethylene-ATP; ATPγS, adenosine 5′-[γ-thio] triphosphate; DDR2, discoidin domain receptor 2; DMEM, Dulbecco's modified Eagle's medium; dNTPs, deoxynucleotide triphosphates; DTT, dithiothreitol; FSK, forskolin; IP, inositol phosphate; MRS 2179, 2-deoxy-N^6-methyl adenosine 3′,5′-diphosphate diammonium salt; MRS 2578, N,N′′-1,4-butanediylbis[N′-(3-isothiocyanatophenyl)thiourea; NF 157, 8,8′-[carbonylbis[imino-3,1-phenylenecarbonylimino(4-fluoro-3,1-phenylene)carbonylimino]]bis-1,3,5-naphthalene trisulphonic acid hexasodium salt; PBS, phosphate-buffered saline; PTX, *Pertussis* toxin; RT-PCR, reverse transcription-polymerase chain reaction

Correspondence: Dr Renée Germack, Biomedical Research Centre, School of Biomedical and Natural Sciences, Nottingham Trent University, Clifton Lane, Nottingham NG11 8NS, UK. E-mail: renee.germack@ntu.ac.uk
Received 9 September 2008; revised 29 October 2008; accepted 23 November 2008

Introduction

P2Y receptors belong to the G protein-coupled receptor super-family, and eight mammalian subtypes [$P2Y_1$, $P2Y_2$, $P2Y_4$, $P2Y_6$, $P2Y_{11}$, $P2Y_{12}$, $P2Y_{13}$ and $P2Y_{14}$; nomenclature follows

Alexander *et al*. (2008)] have been cloned and characterized in different cell types (Abbracchio *et al*., 2006; Von Kügelgen, 2006). P2Y receptors are divided pharmacologically into three groups according to their activation by endogenous adenine and uracil nucleotides. Group I ($P2Y_1$, $P2Y_{11}$, $P2Y_{12}$ and $P2Y_{13}$) is activated by the adenine nucleotides ATP and ADP, group II ($P2Y_6$) stimulated by the uracil nucleotides UTP and UDP, and group III ($P2Y_2$ and $P2Y_4$) responding to both adenine and uracil nucleotides (Abbracchio *et al*., 2006; Von Kügelgen, 2006). The $P2Y_{14}$ receptor is activated by UDP-sugar nucleotides including UDP-glucose (Abbracchio *et al*., 2006; Von Kügelgen, 2006). Most of the P2Y receptors ($P2Y_1$, $P2Y_2$, $P2Y_4$, $P2Y_6$ and $P2Y_{11}$) are coupled to $G_{q/11}$ protein and trigger phospholipase C (PLC) activation followed by the production of inositol phosphates (IPs), whereas $P2Y_{12}$, $P2Y_{13}$ and $P2Y_{14}$ receptors are only coupled to $G_{i/o}$ protein and inhibit adenylyl cyclase (Abbracchio *et al*., 2006; Von Kügelgen, 2006). In addition, $P2Y_2$ and $P2Y_4$ receptors are also coupled to $G_{i/o}$ protein whereas $P2Y_{11}$ activates adenylyl cyclase via G_s protein.

Cardiac fibroblasts are the predominant cell type found in the heart (Camelliti *et al*., 2005). They contribute to myocardial function and structure by secreting growth factors, cytokines and components of the extracellular matrix (ECM) such as collagen and fibronectin (Brown *et al*., 2005; Camelliti *et al*., 2005). As such fibroblasts play an important role in the myocardial remodelling process observed in cardiovascular diseases such as ischaemic heart disease, which involves an increase in ECM, cardiomyocyte hypertrophy, migration and proliferation of fibroblasts (Brown *et al*., 2005). Recent studies have shown that ATP and UTP are released during myocardial infarction in humans (Wihlborg *et al*., 2006). Similarly, Erlinge *et al*. (2005) have shown that the level of UTP increased in porcine heart following cardiac ischaemia. Furthermore, ATP is released from cardiac myocytes and pulmonary artery advential fibroblasts exposed to ischaemia (Gerasimovskaya *et al*., 2002; Dutta *et al*., 2004). These observations suggest that ATP and UTP released during cardiac ischaemia may influence fibroblast function. Previous studies using reverse transcription-polymerase chain reaction (RT-PCR) and Northern blotting have reported the expression of $P2Y_1$, $P2Y_2$, $P2Y_4$ and $P2Y_6$ receptor transcripts in neonatal rat cardiac fibroblasts (Webb *et al*., 1996; Zheng *et al*., 1998). At the functional level, ATP attenuates noradrenaline-induced proliferation and stimulates c-*fos* expression in neonatal rat cardiac fibroblasts (Zheng *et al*., 1998). In addition, ADP, ATP and UTP induce concentration-dependent increases in IP production and augment isoprenaline-induced cAMP accumulation in adult rat cardiac fibroblasts (Meszaros *et al*., 2000).

As cardiac fibroblasts are important in the regulation of ECM and the inflammatory process, extracellular nucleotides acting through P2Y receptors may play an important role during myocardial injury. Indeed, UTP induces cardioprotection by decreasing infarct size and restoring cardiac function in rat heart following myocardial infarction (Yitzhaki *et al*., 2006). Furthermore, $P2Y_2$ receptor mRNA is up-regulated in patients with congestive heart failure (Hou *et al*., 1999). Overall, these studies suggest that extracellular nucleotides and P2Y receptors may play a role in the pathological regulation or adaptation to cardiac diseases and may modulate cardiac fibroblast function by an autocrine and/or paracrine mechanism. However, at present, very little is known about the functional expression of P2Y receptors in cardiac fibroblasts. In addition, cardiac fibroblasts change their phenotype and differentiate into myofibroblasts under certain conditions including growth factor stimuli, mechanical stretch or culture on rigid support (Wang *et al*., 2003; Camelliti *et al*., 2005). The differentiation of cardiac fibroblasts in myofibroblasts leads to the expression of myofilament proteins such as α-smooth muscle actin. Myofibroblasts seem to play an important role in remodelling observed in myocardial infarction (Squires *et al*., 2005). Therefore, the aim of this study was to determine the phenotype of the cells and to characterize the different P2Y receptor subtypes at the expression and functional level in neonatal rat non-cardiomyocytes. We present evidence that $P2Y_1$-, $P2Y_2$-, $P2Y_4$-, $P2Y_6$- and $P2Y_{11}$- like receptors are functionally expressed in myofibroblasts.

Methods

Cell culture

All animal care and experimental procedures complied with the UK Home Office Policy and were approved by the Nottingham Trent University Ethical Committee. Neonatal non-cardiomyocytes were isolated from 1–4-day-old Wistar rats using the Neonatal Cardiomyocyte Isolation System (Worthington Biochemical Corporation, Lornes Laboratories, Reading, UK) as described previously (Germack and Dickenson, 2006). Briefly, hearts were removed from 8–12 neonatal rats killed by cervical dislocation. The ventricles were minced and subjected to trypsin digestion overnight at 4°C. Next day, trypsin was inactivated with soybean trypsin inhibitor for 15 min and then the tissue mixture was digested with collagenase in a shaking water bath for 60 min. Following enzymatic digestion, the cell suspension was filtered through a cell strainer (70 μm), washed and centrifuged. The resulting pellet was resuspended in Dulbecco's modified Eagle's medium (DMEM) supplemented with 10% v/v heat inactivated foetal calf serum, 2 $mmol \cdot L^{-1}$ L-glutamine and penicillin/streptomycin (100 $U \cdot mL^{-1}$). The cells were separated from cardiomyocytes by cellular attachment by using 75 cm^2 flasks for 30 min in a humidified incubator (95% air/5% CO_2 at 37°C). Non-cardiomyocytes were cultured for 6 days in DMEM supplemented with 10% v/v heat inactivated foetal calf serum, 2 $mmol \cdot L^{-1}$ L-glutamine and penicillin/streptomycin (100 $U \cdot mL^{-1}$) until confluence. The cells were subsequently trypsinized, re-seeded in 175 cm^2 flasks and cultured in order to obtain fibroblast rich cultures. After a further 5 days in culture, non-cardiomyocytes were plated on 6-well plates (1×10^6 cells per well) for RT-PCR, 4-well chamber slides (0.06×10^6 cells per well) for immunocytochemistry and 24-well plates (0.15×10^6 cells per well) for cAMP and IP assays. After 3 days in culture, the cells were serum starved overnight before the experiments.

RT-PCR

Total RNA was extracted from non-cardiomyocytes, rat adipose tissue or spleen using the RNA isolation reagent RNAwiz™ (Ambion, Eurotech, Thatcham, UK). Total RNA was

Table 1 Sequences of the primers specific for rat β-actin and $P2Y_1$, $P2Y_2$, $P2Y_4$, $P2Y_6$, $P2Y_{12}$, $P2Y_{13}$ and $P2Y_{14}$ receptors

Primer	*Sequences*	*cDNA (bp)*	*Annealing Temperature (°C)*	*Reference*
β-Actin	Fw: 5′-CGTAAAGACCTCTATGCCAA-3′ Rw: 5′-GGTGTAAAACGCAGCTCAGT-3	301	57	Germack and Dickenson (2006)
$P2Y_1$	Fw: 5′-CATCTCCCCCATTCTCTT-3 Rw: 5′-GTTGCTTCTTCTTGACCTGT-3′	663	57	Hou *et al.* (1999)
$P2Y_2$	Fw: 5′-ACCCGCACCCTCTATTACT-3′ Rw: 5′-CTTAGATACGATTCCCCAACT-3′	538	57	Hou *et al.* (1999)
$P2Y_4$	Fw: 5′-TGGGTGTTTGGTTGGTAGTA-3′ Rw: 5′-GTCCCCCGTGAAGAGATAG-3′	464	57	Hou *et al.* (1999)
$P2Y_6$	Fw: 5′-GTTATGGAGCGGGACAATGG-3′ Rw: 5′-AGGATGCTGCCGTGTAGGTT-3′	347	57	Hou *et al.* (1999)
$P2Y_{12}$	Fw: 5′-TTAAGAACACGGTCATCRCRGATCT-3′ Rw: 5′-TAATTGACTATCTCGTGCCAGACCA-3′	388	57	
$P2Y_{13}$	Fw: 5′-CAGGGACACTCGGATGACA-3′ Rw: 5′-TGTTCGGCAGGGAGATGA-3′	424	57	
$P2Y_{14}$	Fw: 5′-TGTCTGCCGTGATCTTCT-3′ Rw: 5′-GGGTCCAGACACACATTG-3′	589	57	Fumagalli *et al.* (2004)

purified by chloroform/water extraction and isopropanol precipitation. All RNA preparations were treated with RQ1 DNase (1 $U \cdot \mu L^{-1}$) for 20 min at 37°C in the presence of Rnasin (40 $U \cdot \mu L^{-1}$) and dithiothreitol (DTT; 100 $mmol \cdot L^{-1}$). Reverse transcription (RT) was performed with 40 μg total RNA for the synthesis of cDNA by using hexadeoxynucleotide random primers (540 $ng \cdot mL^{-1}$), Rnasin (40 $U \cdot mL^{-1}$), deoxynucleotide triphosphate (dNTP, 5 $mmol \cdot L^{-1}$) and Moloney-murine leukaemia virus reverse transcriptase (200 $U \cdot mL^{-1}$) for 90 min at 42°C. Polymerase chain reaction (PCR) was conducted with 200 ng cDNA for β-actin and 600 ng cDNA for P2Y receptors in the presence of dNTPs (1.25 $mmol \cdot L^{-1}$), 1.5 U *Taq* DNA polymerase and 200 ng of respective primers (Table 1). Following PCR the samples were denatured for 5 min at 95°C, 30 cycles of the amplification steps involved 1 min denaturation at 95°C, 1 min annealing at 57°C and 1 min extension at 72°C. The RT-PCR products were analysed by using 1.5% agarose gel electrophoresis. β-Actin mRNA was used as an internal standard. The RT-PCR products were quantified by densitometry using GeneGenius BioImaging System (Syngene, Synoptics Ltd., Cambridge, UK) and normalized to the signal of β-actin.

Immunocytochemistry

Non-cardiomyocytes were stained by an indirect immunofluorescence method. The cells were washed three times with 1 mL phosphate-buffered saline (PBS), fixed with 200 μL ice cold acetone for 2 min at –20°C and washed a further three times with PBS. To characterize the phenotype and the purity of the cells culture, anti-desmin (Sigma Chemical Co, Poole, UK), α-actin monoclonal (Santa Cruz biotechnology, Santa Cruz, CA, USA) and anti-discoidin domain receptor 2 (DDR2) goat polyclonal antibodies (Santa Cruz biotechnology) were used. Anti-$P2Y_{1,2,4,6,11,13}$ receptor rabbit antibodies and their corresponding control antigen peptides (Alomone Labs/TCS Bioscience, Buckingham, UK) were used to identify P2Y receptors expressed. For the control peptide antigen, primary antibodies ($P2Y_{1,2,4,6,11,13}$: 0.16 mg) and respective peptides (0.08 mg) were pre-incubated for 1 h at 37°C in reagent buffer [3% bovine serum albumin, 0.01% (v/v) Tween 20® in PBS]. Primary antibody–antigen mixture or primary antibody solution was applied for 1 h at 37°C in a humidified chamber, and the cells were washed three times with PBS. Secondary anti-goat immunoglobulin-FITC (Santa Cruz biotechnology), anti-mouse immunoglobulin-FITC (Dako Ltd., Cambridge, UK) or anti-rabbit immunoglobulin-FITC (Dako Ltd.) were incubated for 1 h at 37°C in a humidified chamber, and the cells were washed three times with PBS. For the negative control, the incubation step with primary antibodies was omitted. The slides were mounted with Vectorshield® medium containing propidium iodide (Vector Laboratories Ltd., Peterborough, UK). Non-cardiomyocytes were analysed by using a Leica TCSNT confocal laser microscope system (Leica) equipped with an argon/krypton laser (FITC: E_{495}/E_{278}; propidium iodide: E_{535}/E_{615}).

Inositol phosphate accumulation assay

Non-cardiomyocytes were serum-starved in 500 μL L-15 medium containing [^{3}H]*myo*-inositol (3 μCi per well) for 24 h in a humidified incubator (95% air/5% CO_2 at 37°C). [^{3}H]inositol-labelled cells were washed twice with Hanks/HEPES buffer and then incubated in 500 μL per well serum-free DMEM containing the phosphatase inhibitor LiCl (20 $mmol \cdot L^{-1}$) for 30 min at 37°C in a humidified incubator followed by incubation with agonists for 30 min. Agonists, and/or antagonists or inhibitors were added as described in the figure legends. The potency values for adenine and uracil nucleotides and P2Y receptor antagonists used in the study are summarized in Table 2. Incubations were terminated by the addition of 1 mL ice cold methanol/0.1 $mol \cdot L^{-1}$ HCl (1:1) after removing the medium. Total [^{3}H]inositol phosphates were isolated by sequential Dowex-alumina chromatography as previously described (Dickenson and Hill, 1998). After elution, the levels of [^{3}H]inositol phosphate were determined by liquid scintillation counting.

cAMP accumulation assay

After serum starvation of the cells, assays were carried out in serum-free DMEM in a humidified incubator (95% air/5% CO_2

Table 2 Potency of adenine and uracil nucleotides and antagonists for cloned P2Y receptors

	$P2Y_1$ ($\mu mol \cdot L^{-1}$)	$P2Y_2$ ($\mu mol \cdot L^{-1}$)	$P2Y_4$ ($\mu mol \cdot L^{-1}$)	$P2Y_6$ ($\mu mol \cdot L^{-1}$)	$P2Y_{11}$ ($\mu mol \cdot L^{-1}$)	$P2Y_{12}$ ($\mu mol \cdot L^{-1}$)	$P2Y_{13}$ ($\mu mol \cdot L^{-1}$)
Agonists							
ATP	0.141[a]	0.32[a]	1.0[a]	NA[a]	H: 3.6[b] C: 32.8[b]	M: 0.243[d]	NA[c]
ATPγS			2.1[a]		H: 1.2[b] C: 19.3[b]		
ADPβS	0.096[a]			25.7[a]	H: 3.7[b] C: 0.14[b]	M: 0.007[d]	0.443[c]
2-MeSADP	0.00058[a]			1.7[a]	H: 14.6[b] C: 0.08[b]	0.0009[a] M: 0.006[d]	1.2[c]
2-MeSATP	0.03[a]	NA[a]	2.1[a]	NA[a]	H: 2.4[b] C: 0.57[b]	M: 0.007[d]	NA[c]
UTP		0.79[a]	0.68[a]	0.112[a]	NA[b]		NA[c]
UDP		15.8[a]	4.2[a]	0.019[a]	NA[b]	NA[a]	
Antagonists							
MRS 2179	H: 0.10[e]	H: NA[e]	H: NA[e]	H: NA[e]			NA[c]
MRS 2578	H: NA[f]	H: NA[f]	H: NA[f]	H: 0.037[f], 0.098[f]	H: NA[f]		
NF 157	H: >30[g]	H: >30[g]			H: 0.045[g]		
AR-C69931MX						H: 0.02[h]	0.026[c] H: 0.01[h]

Potency values (as EC_{50}, $\mu mol \cdot L^{-1}$) of the agonists for recombinant rat P2Y receptors, except for the $P2Y_{11}$ receptors that are not cloned yet in this species (H: human, C: canine, M: mouse; NA: no activity).
Antagonist potencies are shown as IC_{50} or –log (pK_B) values. [a]Sak and Webb (2002); [b]Qi *et al.*, 2001; [c]Fumagalli *et al.* (2004); [d]Zhang *et al.* (2002); [e]Boyer *et al.* (1998); [f]Mamedova *et al.* (2004); [g]Ullmann *et al.* (2005); [h]Von Kügelgen (2006).
2-MeSADP, 2(methylthio) adenosine 5′-diphosphate; 2-MeSATP, 2(methylthio) adenosine triphosphate; ADPβS, adenosine 5′-[β-thio]diphosphate; AR-C69931MX, N6-(2-methylthioethyl)-2-(3,3,3-trifluoropropylthio)-β, γ-dichloromethylene-ATP; ATPγS, adenosine 5′-[γ-thio] triphosphate; MRS 2179, 2-deoxy-N^6-methyl adenosine 3′,5′-diphosphate diammonium salt; NF 157, 8,8′-[carbonylbis[imino-3,1-phenylenecarbonylimino(4-fluoro-3,1-phenylene)carbonylimino]]bis-1,3,5-naphthalene trisulphonic acid hexasodium salt.

at 37°C). The cells were incubated for 3 h in a humidified incubator (95% air/5% CO_2 at 37°C) with 500 µL of serum-free DMEM containing [^{3}H]adenine (2 µCi per well). Agonists and/or antagonists or inhibitors were added as described in the figure legends. [^{3}H]adenine-labelled cells were washed twice with Hanks/HEPES buffer and then incubated in 500 µL per well serum-free DMEM containing the cAMP phosphodiesterase inhibitor rolipram (10 $\mu mol \cdot L^{-1}$) for 15 min at 37°C in a humidified incubator. Agonists were added 5 min prior to the incubation with 1.5 $\mu mol \cdot L^{-1}$ forskolin (10 min). Incubations were terminated by the addition of 500 µL 5% (w/v) trichloroacetic acid after removing the medium. [^{3}H]cAMP was isolated by sequential Dowex-alumina chromatography as previously described (Germack and Dickenson, 2006). After elution, the levels of [^{3}H]cAMP were determined by liquid scintillation counting.

Statistical analysis
Results are expressed as means ± SE. Concentration–response and inhibition–response curves were analysed by computer-assisted iteration using the GraphPad Prism (GraphPad Software, San Diego, USA). Statistical significance was determined by analysis of variance (ANOVA) followed by Bonferroni test, and $P < 0.05$ was considered as the limit of statistical significance.

Materials
Adenosine, AMP, ADPβS (adenosine 5′-[β-thio]diphosphate), 2-MeSADP [2(methylthio) adenosine 5′-diphosphate], ATP, ATPγS (adenosine 5′-[γ-thio] triphosphate), UDP, UTP, MRS 2179 (2-deoxy-N^6-methyl adenosine 3′,5′-diphosphate diammonium salt), forskolin, *Pertussis* toxin (PTX) and rolipram were obtained from Sigma Chemical Co. (Poole, U.K.). 2-MeSATP [2(methylthio) adenosine triphosphate], MRS 2578, NF 157 (8,8′-[carbonylbis[imino-3,1-phenylenecarbonylimino(4-fluoro-3,1-phenylene)carbonylimino]]bis-1,3,5-naphthalene trisulphonic acid hexasodium salt) were purchased from Tocris (Bristol, UK). [2,8-^{3}H]-adenine and [2-^{3}H]-*myo*-inositol were from Amersham International (Aylesbury, Bucks, UK) and MP Biomedicals Inc. (CA, USA) respectively. All molecular biology reagents including RQ1 RNase-free DNase, M-MLV reverse transcriptase and random primers were obtained from Promega (Southampton, UK). Primers for RT-PCR analysis were synthesized by Sigma-Genosys (Pampisford, Cambridgeshire, UK). DMEM, foetal calf serum, trypsin (10×), L-glutamine (200 $mmol \cdot L^{-1}$) and penicillin (10 000 $U \cdot mL^{-1}$)/streptomycin (10 000 $\mu g \cdot mL^{-1}$) were purchased from BioWhittaker (Wokingham, UK). The specific $G_{q/11}$ protein blockers YM-254890 (YM) and AR-C69931MX [N6-(2-methylthioethyl)-2-(3,3,3-trifluoropropylthio)-β, γ-dichloromethylene-ATP] were a generous gift from Professor Taniguchi (Yamanouchi Pharmaceutical Co., Ltd., Japan) and AstraZeneca respectively.

Results

Phenotypic characterization of neonatal rat cardiac cell culture
Discoidin domain receptor 2 is a specific marker for cardiac fibroblasts (Goldsmith *et al.*, 2004). Endothelial cells and smooth muscles cells may be present in the cell culture; however, they do not express DDR2. A characteristic of

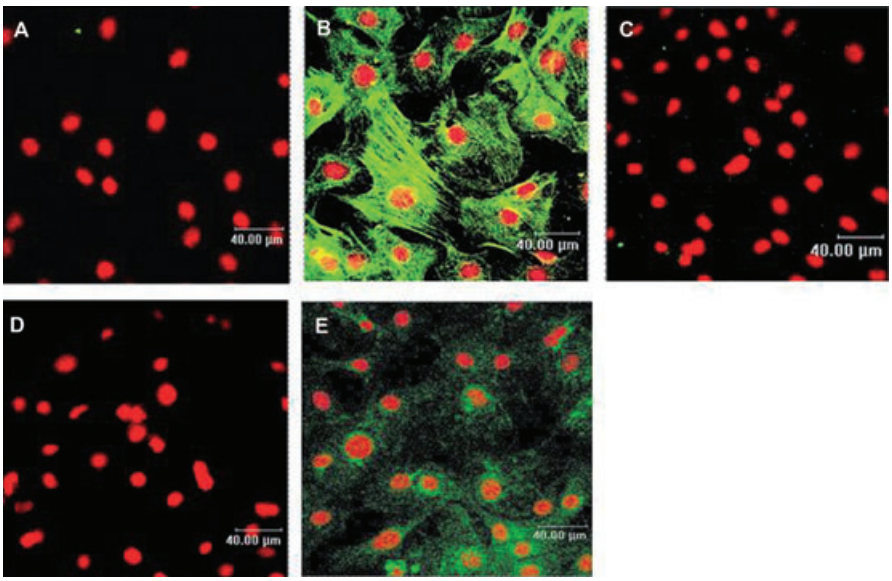

Figure 1 Phenotypic characterization of neonatal rat non-cardiomyocyte cell culture by immunocytochemistry. Immunocytochemistry by confocal microscopy was performed as described under *Materials* and *Methods* using specific α-actin, desmin and discoidin domain receptor 2 (DDR2) antibodies (green). Nuclei were stained with propidium iodide (red). Panels (B, C and E) represent confocal images of α-actin, desmin and DDR2 respectively. Controls were performed in the absence of the primary antibody and in the presence of the secondary rabbit anti-mouse (panel A) and donkey anti-goat (panel D). Images presented are from one experiment and representative of three.

fibroblasts is their ability to differentiate into myofibroblasts, which express not only DDR2 but also myofilament proteins such as α-smooth muscle actin (Wang *et al.*, 2003; Squires *et al.*, 2005). In addition, neonatal rat fibroblasts acquire a myofibroblast phenotype following 3 days in culture (Wang *et al.*, 2003) indicating that the cells used in our study are more likely differentiated cardiac fibroblasts. Desmin is an intermediate filament protein expressed in smooth and cardiac muscles but not in fibroblasts or myofibroblasts (Paulin and Li, 2003; Wang *et al.*, 2003). Therefore, we investigated the expression of DDR2, α-actin and desmin by confocal microscopy in order to determine the phenotype of the non-cardiomyocyte cells used in our study. As shown in Figure 1, the cells expressed α-actin and DDR2 but not desmin indicating that fibroblasts are differentiated into myofibroblasts. In addition, they represented the major cell type (>95%) in our culture conditions. Therefore, the characterization of the P2Y receptors below was investigated in neonatal rat cardiac myofibroblasts.

Expression of P2Y receptors by RT-PCR and confocal microscopy in neonatal rat myofibroblasts

The expression of mRNA encoding for $P2Y_1$, $P2Y_2$, $P2Y_4$, $P2Y_6$, $P2Y_{12}$, $P2Y_{13}$ and $P2Y_{14}$ receptors was investigated in serum-starved neonatal rat myofibroblasts by RT-PCR analysis (Figure 2). Although a $P2Y_{11}$-like receptor is reported to be functionally expressed in mice cardiomyocytes and rat smooth muscle cells (Balogh *et al.*, 2005; Chootip *et al.*, 2005), we could not determine $P2Y_{11}$ mRNA expression as the rodent subtype has not yet been cloned. $P2Y_1$, $P2Y_2$, $P2Y_4$, $P2Y_6$ and $P2Y_{13}$ were expressed in myofibroblasts whereas the expression of $P2Y_{12}$ and $P2Y_{14}$ was not observed in these cells. The absence of these P2Y receptors in myofibroblasts was confirmed by using brown adipose tissue and spleen, which expressed $P2Y_{12}$ and $P2Y_{14}$ receptors respectively (Lee *et al.*, 2005; Scrivens and Dickenson, 2005). To further characterize the expression of P2Y receptor subtypes, immunostaining was performed by using $P2Y_1$, $P2Y_2$, $P2Y_4$, $P2Y_6$, $P2Y_{11}$ and $P2Y_{13}$ antibodies. The anti-human $P2Y_{11}$ antibody displays reactivity with rat spleen and lung as shown by the manufacturer and with Neuro2a cells (Lakshmi and Joshi, 2006). Immunofluorescence was detected for all the receptors expressed at mRNA level using RT-PCR (Figure 3). No staining was observed in the presence of the peptide antigen (Figure 3B,D,F,H,J,L) or in the absence of the primary antibody (Figure 3M). Overall, these data suggest that neonatal rat myofibroblasts express $P2Y_1$, $P2Y_2$, $P2Y_4$, $P2Y_6$ receptors as previously shown in cardiac fibroblasts (Webb *et al.*, 1996) in addition to $P2Y_{11}$ and $P2Y_{13}$ subtypes.

Effect of adenine and uracil nucleotides on inositol phosphate accumulation in neonatal rat myofibroblasts

Most of the P2Y receptors ($P2Y_1$, $P2Y_2$, $P2Y_4$, $P2Y_6$, $P2Y_{11}$) are $G_{q/11}$ protein-coupled receptors linked to PLC (Abbracchio *et al.*, 2006). Therefore, we investigated the effect of adenine and uracil nucleotides on IP accumulation. Both adenine and uracil nucleotides increased IP production in a concentration-dependent manner (Figure 4; Table 3). ATPγS (a stable analogue of ATP) was more potent than ATP with a higher maximal response (38%, ATPγS vs. ATP; Figure 4A; Table 3). The effects of adenosine and ATP in the presence of alloxazine (A_{2B} adenosine receptor antagonist) were investigated to assess the possibility that ATP-induced IP production involved its breakdown into adenosine. This issue is important as rat cardiac fibroblasts express the A_{2B} adenosine receptor (Dubey *et al.*, 1998; Fredholm *et al.*, 2001). As shown in Figure 5C, the

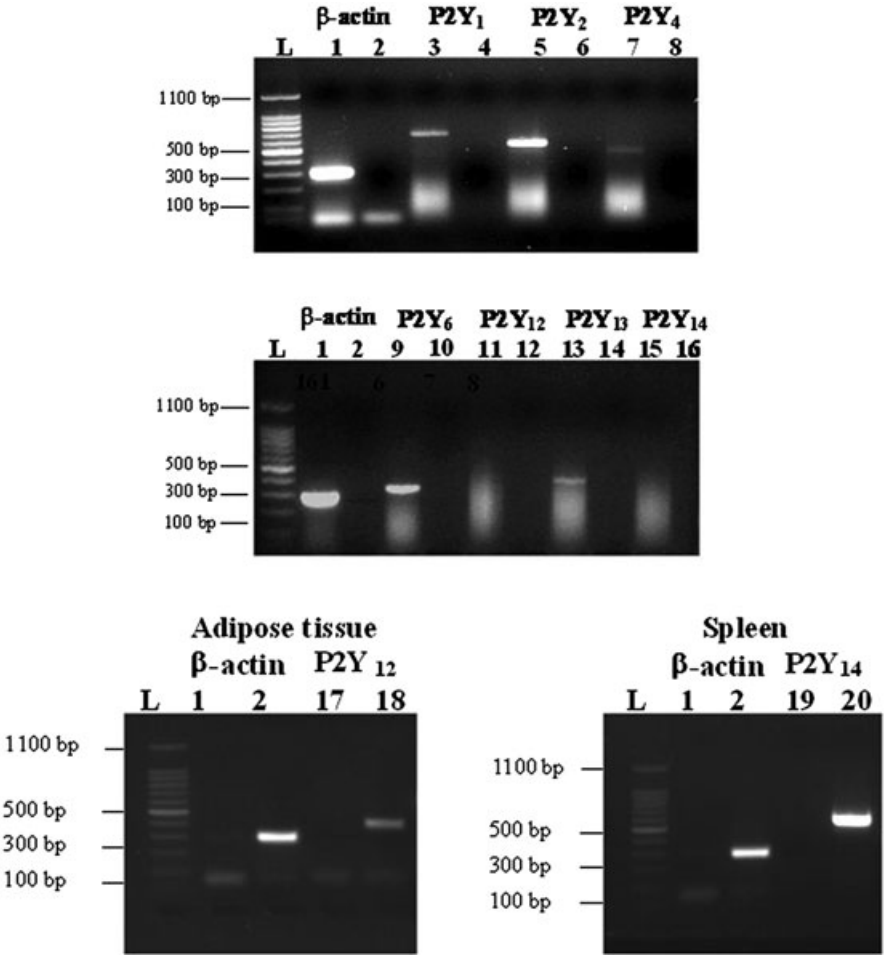

Figure 2 Expression of P2Y receptor mRNA obtained from neonatal rat cardiac myofibroblasts. Total RNA was prepared and reverse transcription-polymerase chain reaction was carried out as described under *Materials* and *Methods*; 1.5% agarose gel electrophoresis represent mRNA coding for β-actin (lanes 1–2), $P2Y_1$ (lanes 3–4), $P2Y_2$ (lanes 5–6), $P2Y_4$ (lanes 7–8), $P2Y_6$ (lanes 9–10), $P2Y_{12}$ (lanes 11–12, 17–18 in brown adipose tissue), $P2Y_{13}$ (lanes 13–14) and $P2Y_{14}$ (lanes 15–16 and 19–20 in spleen). Lanes 2, 4, 6, 8, 10, 12, 14, 16 in myofibroblasts, lanes 1 and 17 in adipose tissue and lanes 1 and 19 in spleen correspond to the primer control without cDNA and lane L to the ladder. Gel images presented are from one experiment and representative of seven independent experiments for myofibroblasts and three for brown adipose tissue and spleen.

A_{2B} receptor antagonist inhibited adenosine-induced cAMP accumulation by 80 ± 9% with an EC_{50} of 557 nmol·L^{-1} (pEC_{50} 6.25 ± 0.24, $n = 3$) indicating that myofibroblasts express mainly the A_{2B} receptor and adenosine triggers its effect mostly through the stimulation of this subtype. Indeed, less than 20% of the adenosine response was resistant to alloxazine indicating that A_{2A} receptors may be involved in adenosine-induced cAMP accumulation and suggesting a low expression of this subtype. Adenosine induced a marked inhibition of the basal IP accumulation, and ATP in the presence of the A_{2B} receptor antagonist exhibited a greater maximal response than obtained with ATP alone (Figure 4A; Table 3). All together, these data indicate that ATP is degraded into adenosine. AMP also induced a similar inhibition of basal IP accumulation. In contrast, ADPβS, 2-MeSADP and 2-MeSATP triggered small (around 35%) but significant increases in IP response (Figure 3A and C; Table 3). Finally, the uracil nucleotides UDP and UTP stimulated robust increases in IP production (Figure 4D; Table 3). Interestingly, UDP-induced IP accumulation was significantly biphasic, and both components elicited a similar maximal response. The rank order of agonist potency to induce IP accumulation was 2-MeSADP > 2-MeSATP ≈ ADPβS > UDP (component-I) > UTP > ATPγS > UDP (component-II) > ATP. We did not perform functional studies with the $P2Y_{14}$ agonist UDP-glucose as this subtype was not detected in myofibroblasts (Figure 2).

Effect of adenine and uracil nucleotides on cAMP accumulation in neonatal rat myofibroblasts

P2Y receptors stimulate intracellular cAMP production via G_s protein coupling ($P2Y_{11}$) or inhibit cAMP accumulation via G_i protein-coupled $P2Y_2$, $P2Y_4$, $P2Y_6$, $P2Y_{12}$, $P2Y_{13}$ and $P2Y_{14}$ receptors (Abbracchio *et al.*, 2006). Therefore we determined the effect of adenine and uracil nucleotides on cAMP accumulation in neonatal rat myofibroblasts.

ATP, ATPγS and ADPβS induced significant increases in cAMP accumulation (Figure 5A; Table 3). As found with IP accumulation, ATPγS was more potent than ATP, with an

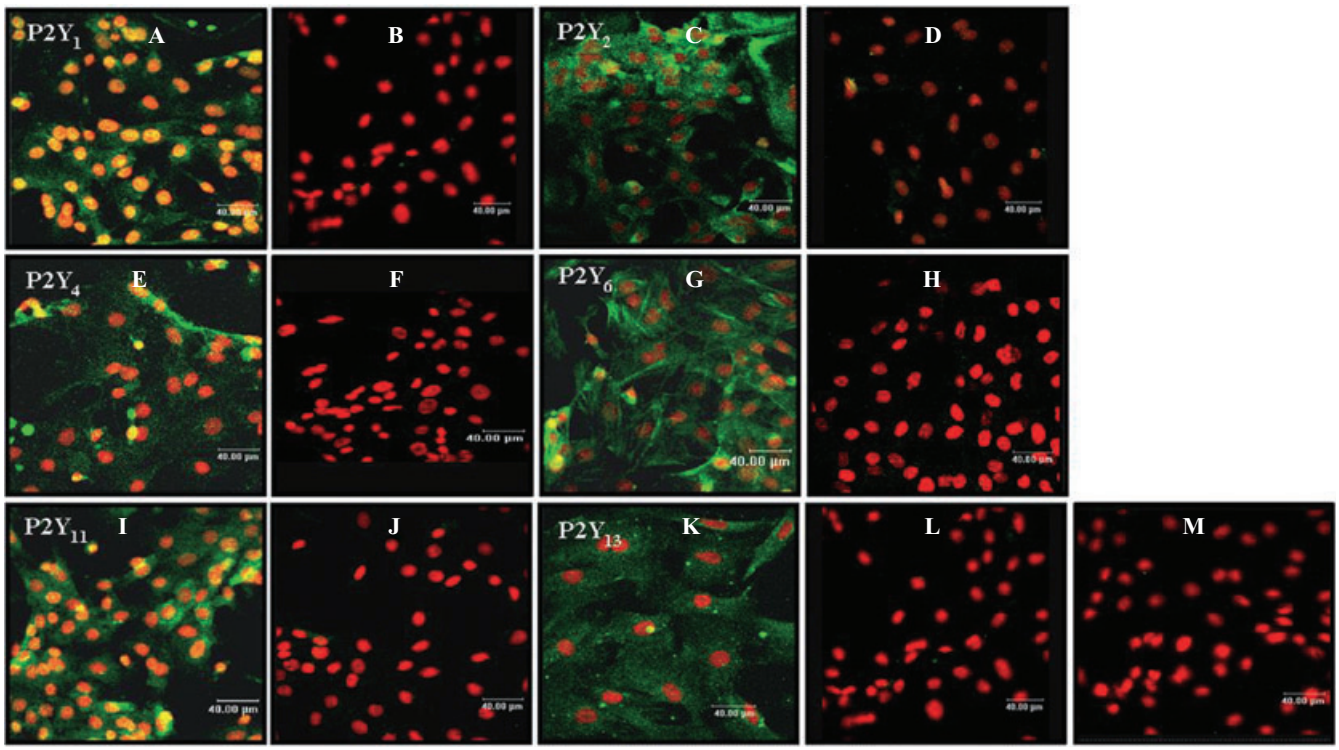

Figure 3 Expression of P2Y receptors in neonatal rat cardiac myofibroblasts by immunocytochemistry. Immunocytochemistry by confocal microscopy was performed as described under *Materials* and *Methods* by using specific P2Y receptor antibodies (green). Nuclei were stained with propidium iodide (red). Panels (A-B, C-D, E-F, G-H, I-J and K-L) represent confocal images of $P2Y_1$, $P2Y_2$, $P2Y_4$, $P2Y_6$, $P2Y_{11}$ and $P2Y_{13}$ respectively. Controls were performed in the presence of the immunogenic peptide for each receptor (panels B, D, F, H, J and L) or in the absence of the primary antibody (panel M). Images presented are from one experiment and representative of 4.

E_{max} twofold higher than the ATP response ($P < 0.01$). The presence of alloxazine increased ATP-induced cAMP accumulation by around 50% (Figure 5A; Table 3) compared with ATP alone, indicating the breakdown of ATP into adenosine. Interestingly, AMP induced the highest response in cAMP accumulation (Figure 5A; Table 3). Although Gao *et al*. (2007) suggest an excitatory action of AMP via A_{2A} receptors in submucosal neurons, AMP-induced cAMP accumulation is unlikely to be mediated by A_{2A} receptor stimulation in cardiac myofibroblasts, as there is thought to be a low functional expression of this subtype (see above), and the high level of AMP response, which represents six times adenosine-induced cAMP production. The rank order of agonist potency to induce cAMP accumulation was ATPγs ≈ ADPβS ≈ adenosine > AMP > ATP suggesting the involvement of a $P2Y_{11}$-like receptor. No cAMP accumulation was observed in response to 2-MeSADP, 2-MeSATP, UDP and UTP (data not shown), indicating that these nucleotides do not activate the G_s pathway in myofibroblasts. In order to investigate their possible stimulation of the $G_{i/o}$ pathway, we determined the effect of 2-MeSADP, 2-MeSATP and uracil nucleotides on forskolin-stimulated cAMP accumulation. No response was observed with 2-MeSADP and 2-MeSATP (data not shown) indicating that the receptor(s) stimulated by these agonists are not coupled to G_i or G_s. In contrast, UDP and UTP produced an inhibition of forskolin-stimulated cAMP accumulation (Figure 5B; Table 3) suggesting that the uracil nucleotides activate $G_{i/o}$ protein through $P2Y_2$, $P2Y_4$ and/or $P2Y_6$ receptors. The maximal inhibition–response induced by UTP was 38% higher than UDP-mediated inhibition of forskolin response.

Effect of selective P2Y receptor antagonists on adenine and uracil induced IP and cAMP accumulation in neonatal rat myofibroblasts

The functional characterization of P2Y receptor expression is severely hampered by the lack of selective P2Y receptor agonists and antagonists. However, we investigated the functional expression of the different subtypes by using the selective antagonists available. We determined the effect of the selective antagonists for $P2Y_1$ receptors (MRS 2179; Boyer *et al*., 1998), $P2Y_6$ receptors (MRS 2578; Mamedova *et al*., 2004), $P2Y_{11}$ receptors (NF 157; Ullmann *et al*., 2005) and a selective antagonist of both $P2Y_{12}$ (Gachet, 2005) and $P2Y_{13}$ receptors (AR-C69931MX; Marteau *et al*., 2003). For these studies we used a concentration of agonist corresponding to 10 times the EC_{50} value (Table 3).

The selective antagonist of $P2Y_1$ receptors, MRS 2179, blocked ADPβS- and 2-MeSADP-mediated IP production by around 40% in addition to ATPγS- and UTP-induced responses by around 20% (Figure 6A and B; Table 4). It is noteworthy that MRS 2179 also blocks $P2X_1$ and $P2X_3$ ion-channel receptors (Brown *et al*., 2000). In addition, these P2X subtypes are activated by UTP and expressed in rat heart (Froldi *et al*., 1997; Hansen *et al*., 1999). Therefore, the partial inhibition of

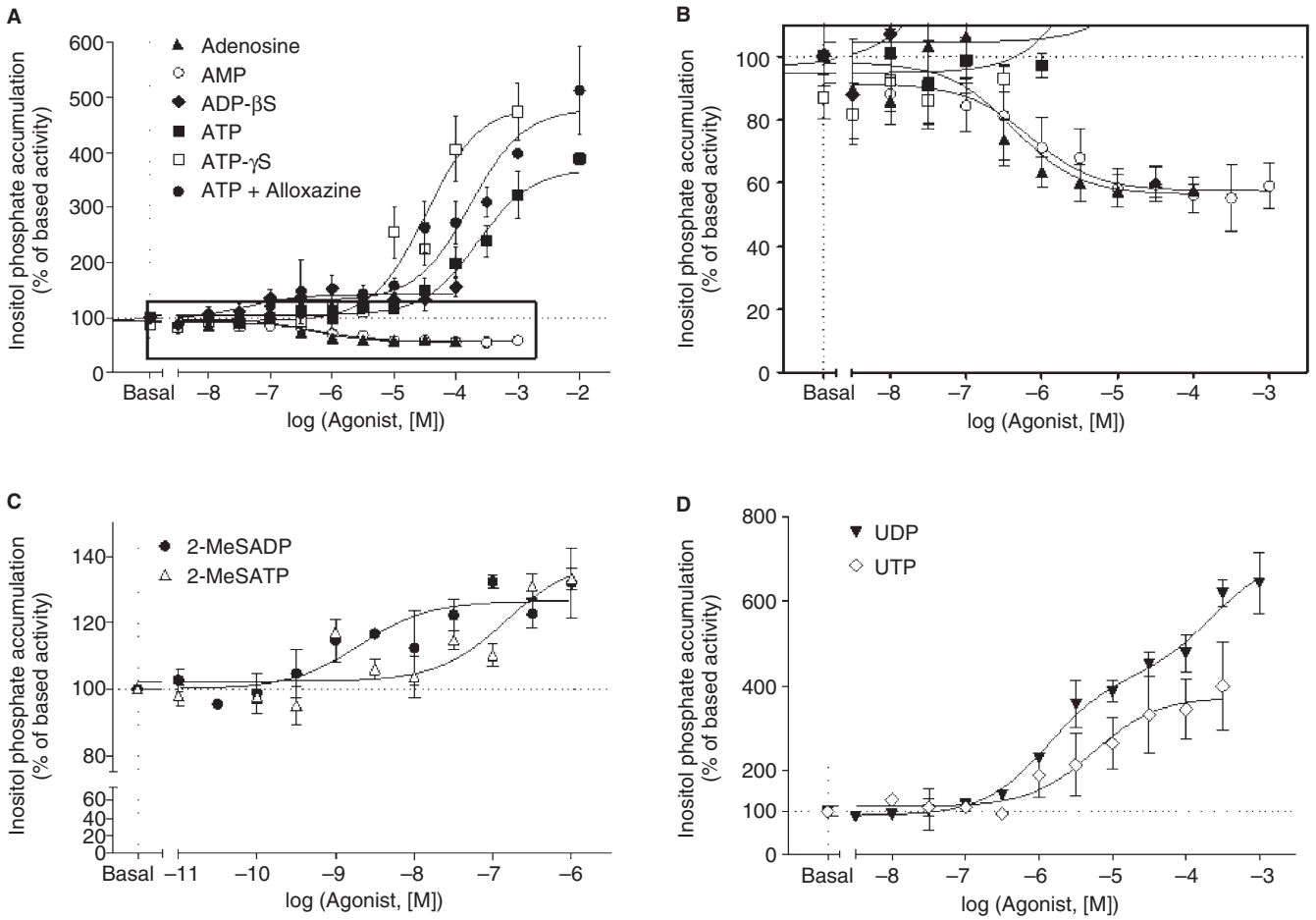

Figure 4 Effect of adenine and uracil nucleotides on inositol phosphate accumulation (IP) in neonatal rat cardiac myofibroblasts. IP accumulation was measured as described under *Materials* and *Methods*. Cardiac myofibroblasts were stimulated with adenosine, AMP, ADPβS (adenosine 5′-[β-thio]diphosphate), ATP, ATP + alloxazine and ATPγS (adenosine 5′-[γ-thio] triphosphate) in panel (A), 2-MeSADP [(methylthio) adenosine 5′-diphosphate] and 2-MeSATP [2(methylthio) adenosine triphosphate] in panel (C), and UDP and UTP in panel (D). Panel (B) corresponds to the enlargement of the frame in panel (A). Data are expressed as percentage of basal IP level (100%) and represent the mean ± SE of three to six independent experiments each performed in duplicate.

UTP-induced IP accumulation by the $P2Y_1$ selective antagonist may involve the inhibition of $P2X_1$ and/or $P2X_3$ receptors. MRS 2179 had no effect on AMP-, 2-MeSATP- and UDP-induced IP responses (data not shown). The rank order of MRS 2179 potency to antagonize agonist-induced IP accumulation was ADPβS ≈ ATPγS > 2MeSADP > UTP. Furthermore, MRS 2179 did not block AMP-, ADPβS- and ATPγS-activated cAMP accumulation or UDP- and UTP-mediated inhibition of forskolin response (data not shown) indicating that the $P2Y_1$ subtype is only coupled to $G_{q/11}$ protein.

The $P2Y_6$ receptor antagonist, MRS 2578, inhibited ATPγS, UDP- and UTP-mediated IP accumulation with a similar potency (Figure 6C and D; Table 4). Interestingly, MRS 2578 displayed a bell-shaped inhibition curve with ATPγS and UDP. This shape of curve may reflect a positive cooperative interaction between at least two receptors as shown with angiotensin receptors (Moore and Scanlon, 1989). On the basis of the formation of receptor dimers, the antagonist MRS 2578 by inhibiting preferentially one subtype may induce an increase in agonist potency for the second receptor, and therefore enhance IP accumulation induced by the former subtype, which is antagonized at high antagonist concentration. Indeed, MRS 2578 potentiated ATPγS and UDP response at concentrations below 316 nmol·L^{-1} whereas above this concentration, MRS 2578 inhibited ATPγS- and UDP-induced IP accumulation. In addition, the concentration inhibition curves with ATP and UDP was best fitted by a two-site model ($P < 0.001$ and $P < 0.01$, respectively) strengthening the idea that UDP stimulates at least two different P2Y receptor subtypes, which are able to interact with each other as observed with the concentration–response curve (Figure 4D). The activation of cAMP by ATPγS was not blocked by MRS 2578 (data not shown). Furthermore, this antagonist did not modify UDP- and UTP-mediated inhibition of forskolin response (data not shown). Overall, these results suggest that $P2Y_6$ receptor-induced responses involve only $G_{q/11}$ protein coupling.

As shown in Figure 7, the $P2Y_{11}$ receptor antagonist NF 157 inhibited ADPβS-induced IP accumulation (I_{max}: 64 ± 11%; pIC_{50}: 9.04 ± 0.32, $n = 3$) but surprisingly had no effect on ATPγS responses (data not shown). Similarly NF 157 did not inhibit ADPβS- or ATPγS-induced cAMP responses (data

Table 3 Effect of adenine and uracil nucleotides on inositol phosphate and cAMP accumulation in neonatal rat fibroblasts

Agonist	*[³H]cAMP accumulation*				*[³H]inositol phosphate*			
	EC_{50}	E_{max}	IC_{50}	I_{max}	EC_{50}	E_{max}	IC_{50}	I_{max}
Adenosine	5.2 ± 0.4 (6.3)	112 ± 23					6.1 ± 0.1 (0.79)	39 ± 10
AMP	4.9 ± 0.1 (12.5)	676 ± 152					6.2 ± 0.4 (0.63)	36 ± 4
ADPβS	5.3 ± 0.4 (5.0)	94 ± 39			7.2 ± 0.2 (0.06)	39 ± 7		
ATP	4.7 ± 0.4 (19.9)	128 ± 37			3.5 ± 0.2 (316.2)	322 ± 50		
ATPγS	5.4 ± 0.2 (3.9)	247 ± 53			4.5 ± 0.1 (31.6)	444 ± 62		
ATP + Alloxazine	3.7 ± 0.2 (169)	287 ± 22			3.8 ± 0.2 (172)	479 ± 35		
2-MeSATP	NR	NR			7.1 ± 0.4 (0.07)	34 ± 4		
2-MeSADP	NR	NR			8.5 ± 0.8 (0.003)	33 ± 7		
UDP	NR	NR	4.9 ± 0.5 (10)	51 ± 15	Receptor I[a]: 5.8 ± 0.2 (1.5)	Receptor I: 329 ± 29		
					Receptor II: 3.6 ± 0.0 (251.1)	Receptor II: 291 ± 31		
UTP	NR	NR	5.4 ± 0.3 (3.98)	82 ± 16	5.2 ± 0.2 (6.3)	345 ± 110		

Values are means ± SEM from 3–7 experiments performed in duplicate. The potencies of the agonists were evaluated by their EC_{50} (concentration of agonist inducing 50% of the maximal response) or their IC_{50} (concentration of agonist inducing 50% of inhibition), expressed as $-\log_{10}$ EC_{50} or $-\log_{10}$ IC_{50} respectively. E_{max} is the maximal response expressed in percentage over basal response. I_{max} is the maximal percentage of inhibition. The values in parenthesis represent the EC_{50} or IC_{50} in µmol·L^{-1}.
NR means no response. [a]corresponds to data, which was best fitted by a two-site model (***$P < 0.001$).
2-MeSADP, 2(methylthio) adenosine 5′-diphosphate; 2-MeSATP, 2(methylthio) adenosine triphosphate; ADPβS, adenosine 5′-[β-thio]diphosphate; AR-C69931MX, N6-(2-methylthioethyl)-2-(3,3,3-trifluoropropylthio)-β, γ-dichloromethylene-ATP; ATPγS, adenosine 5′-[γ-thio] triphosphate; MRS 2179, 2-deoxy-N^6-methyl adenosine 3′,5′-diphosphate diammonium salt.

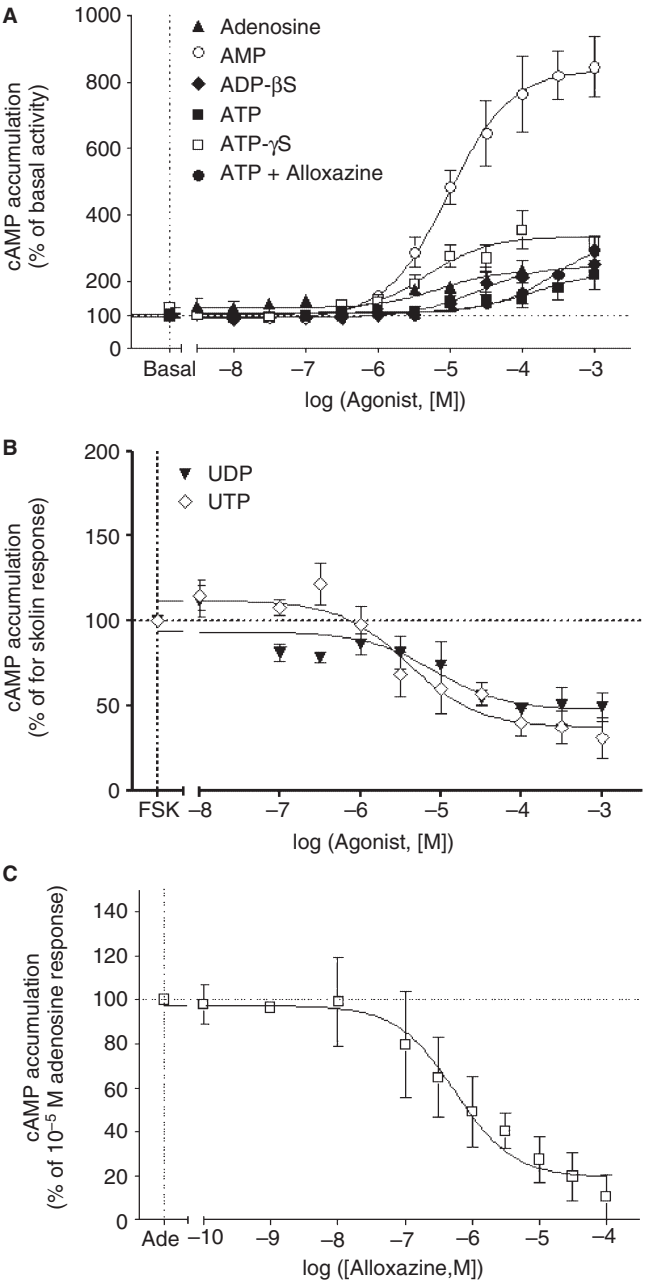

Figure 5 Effect of adenine and uracil nucleotides on cAMP accumulation and effect of alloxazine on adenosine-induced cAMP accumulation in neonatal rat cardiac myofibroblasts. cAMP accumulation was measured as described in *Methods*. Cardiac myofibroblasts were stimulated with adenosine, AMP, ADPβS (adenosine 5′-[β-thio]diphosphate), ATP, ATP + alloxazine and ATPγS (adenosine 5′-[γ-thio] triphosphate) in panel (A), and UDP and UTP in panel (B). Cardiac myofibroblasts were incubated with the indicated concentrations of alloxazine for 30 min before stimulating with 10 µmol·L^{-1} adenosine (panel C). Data in panel (A) are expressed as percentage of basal cAMP accumulation (100%) and represent the mean ± SE of three to six independent experiments each performed in duplicate. Data in panel (B) are expressed as the percentage of 1.5 µmol·L^{-1} forskolin response (100%) and represent the mean ± SE of three to seven independent experiments each performed in duplicate. Data in panel (C) are expressed as the percentage of the adenosine-induced cAMP accumulation in the absence of antagonist (100%) and represent the mean ± SE of three independent experiments performed in duplicate.

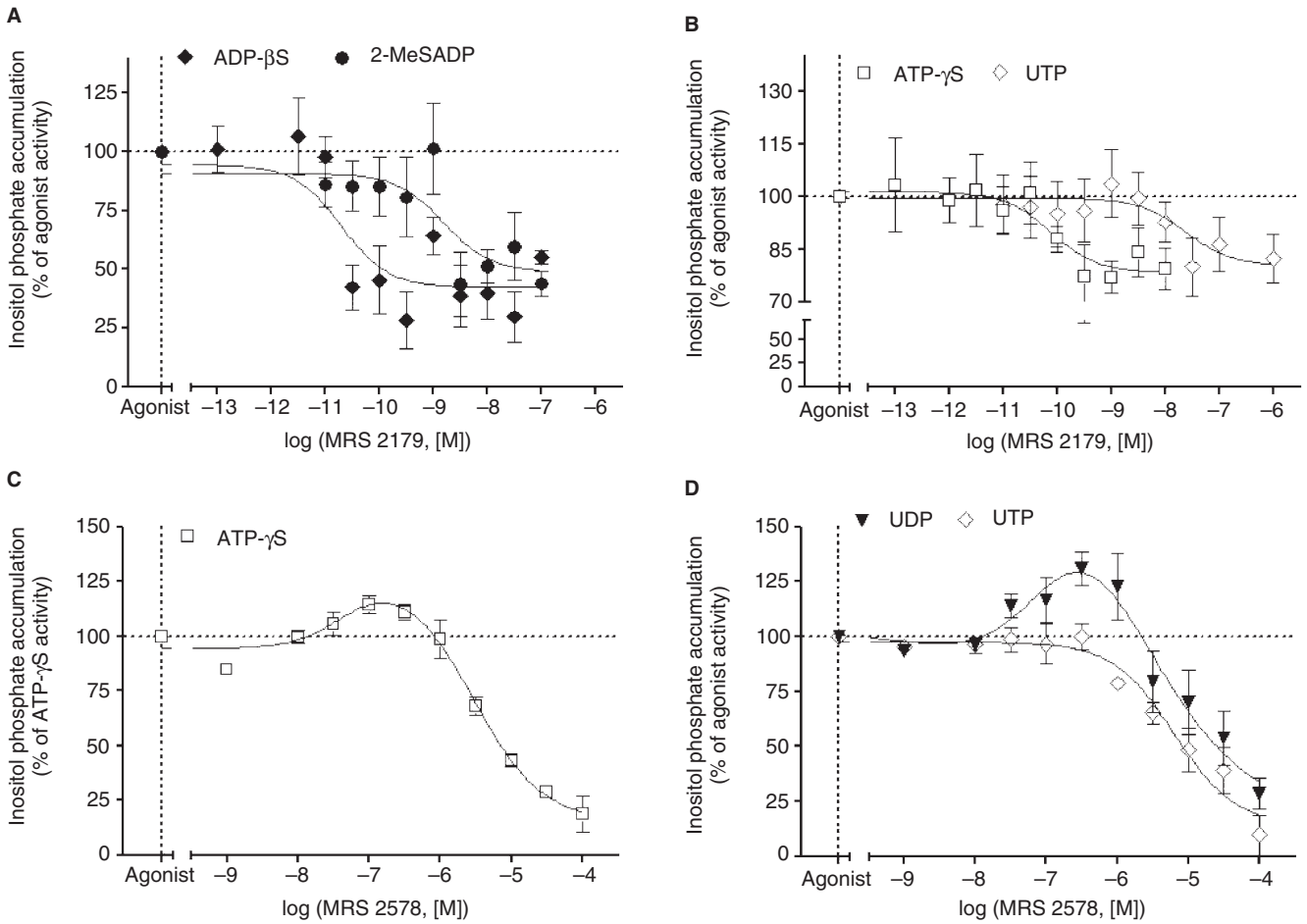

Figure 6 Effect of MRS 2179 (2-deoxy-N^6-methyl adenosine 3′,5′-diphosphate diammonium salt) and MRS 2578 on adenine and uracil nucleotides-induced inositol phosphate (IP) accumulation in neonatal rat cardiac myofibroblasts. Cardiac myofibroblasts were incubated with the indicated concentrations of MRS 2179 for 30 min before stimulating with 1 μmol·L^{-1} ADPβS (adenosine 5′-[β-thio]diphosphate) and 0.1 μmol·L^{-1} 2-MeSADP [2(methylthio) adenosine 5′-diphosphate] (panel A), 100 μmol·L^{-1} ATPγS (adenosine 5′-[γ-thio] triphosphate) and 100 μmol·L^{-1} UTP for 30 min (panel B). Cardiac myofibroblasts were incubated with the indicated concentrations of MRS 2578 (N,N′′-1,4-butanediylbis[N′-(3-isothiocyanatophenyl)thiourea) for 30 min before stimulating with 100 μmol·L^{-1} ATPγS (panel C) and 100 μmol·L^{-1} UDP and 100 μmol·L^{-1} UTP for 30 min (panel D). ADPβS, ATPγS, 2-MeSADP, UDP and UTP induced an increase of IP accumulation of 40%, 440%, 33%, 450% and 375% above basal activity. Data are expressed as the percentage of the agonist-induced IP accumulation in the absence of antagonist (100%) and represent the mean ± SE of three to six independent experiments performed in duplicate.

Table 4 Effect of MRS 2179 and MRS 2578 on adenine and uracil nucleotides-induced inositol phosphate accumulation in neonatal rat cardiac fibroblasts

Agonist	*MRS 2179 ($P2Y_1$ antagonist)*		*MRS 2578 ($P2Y_6$ antagonist)*			
			1		*2*	
	I_{max}	IC_{50}	E_{max}	EC_{50}	I_{max}	IC_{50}
ADPβS	48 ± 5	10.7 ± 0.4 (0.019)				
ATPγS	23 ± 1	10.1 ± 0.4 (0.079)	18 ± 2	7.6 ± 0.1 (25.1)	84 ± 7	5.4 ± 0.1 (3980)
2-MeSADP	40 ± 9	8.8 ± 0.6 (1.58)				
UTP	20 ± 2	7.6 ± 0.7 (25.1)			87 ± 11	5.1 ± 0.1 (7940)
UDP	NR	NR	35 ± 6	7.3 ± 0.1 (50.1)	71 ± 6	5.3 ± 0.2 (5010)

Values are means ± SE of 3–6 experiments performed in duplicate. The potencies of the antagonists were evaluated by their IC_{50} (concentration of antagonist inducing 50% of inhibition), expressed as $-\log_{10}$ IC_{50}. I_{max} is the maximal percentage of inhibition. With MRS 2578 (N,N′′-1,4-butanediylbis[N′-(3-isothiocyanatophenyl)thiourea), the potencies of the component 1 were evaluated by their EC_{50} (concentration of agonist inducing 50% of maximal response), as $-\log_{10}$ EC_{50}. E_{max} is the maximal response expressed in percentage over basal response. The values in parenthesis represent the IC_{50} in nmol·L^{-1}. NR means no response.

2-MeSADP, 2(methylthio) adenosine 5′-diphosphate; ADPβS, adenosine 5′-[β-thio]diphosphate; ATPγS, adenosine 5′-[γ-thio] triphosphate; MRS 2179, 2-deoxy-N^6-methyl adenosine 3′,5′-diphosphate diammonium salt.

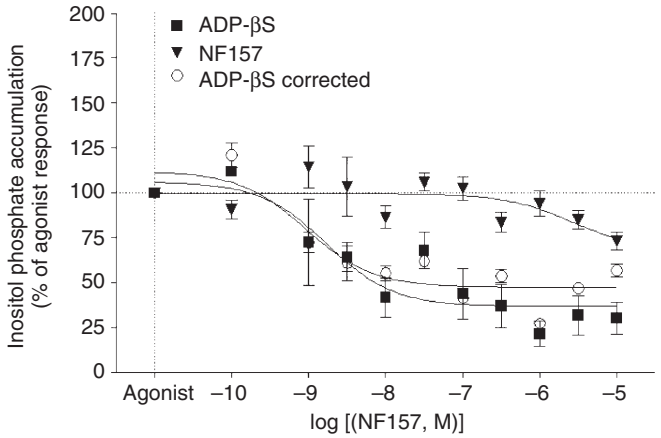

Figure 7 Effect of NF 157 [8,8′-[carbonylbis[imino-3,1-phenylene-carbonylimino(4-fluoro-3,1-phenylene)carbonylimino]]bis-1,3,5-naphthalene trisulphonic acid hexasodium salt] on adenosine 5′-[β-thio]diphosphate (ADPβS)-induced inositol phosphate (IP) response in neonatal rat cardiac myofibroblasts. Cardiac myofibroblasts were incubated with the indicated concentrations of NF 157 for 60 min alone and for 30 min before stimulating with 1 μmol·L^{-1} ADPβS. The effect of NF 157 on IP accumulation was removed from the response to ADPβS. Data are expressed as the percentage of the agonist-induced IP accumulation in the absence of antagonist (100%) and represent the mean ± SE of three independent experiments performed in duplicate.

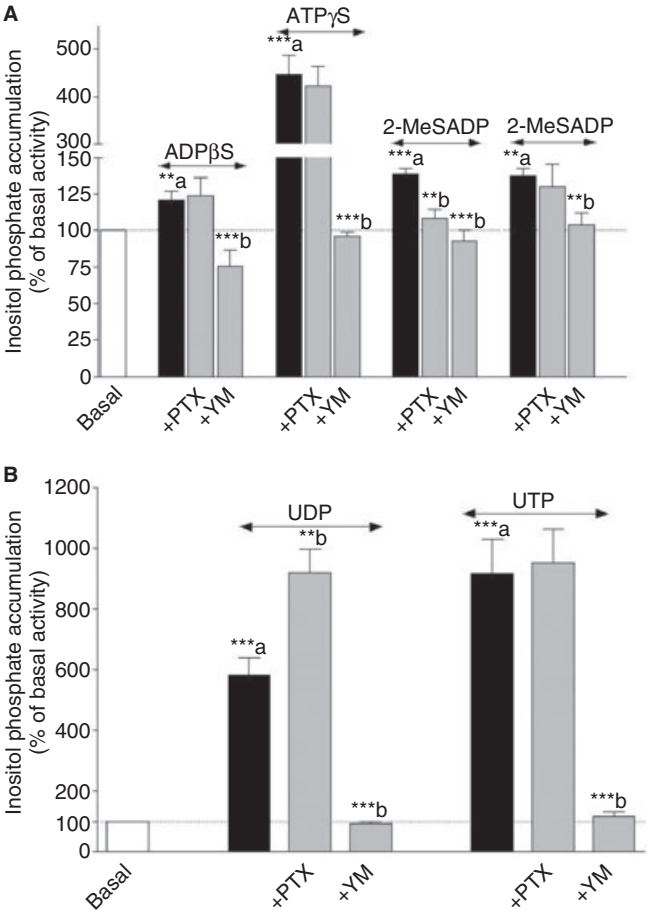

Figure 8 Effect of *Pertussis* toxin (PTX) and YM 254890 (YM) on adenine (panel A) and uracil (panel B) nucleotides-induced inositol phosphate (IP) accumulation in neonatal rat cardiac myofibroblasts. Cardiac myofibroblasts were pretreated with 100 ng·mL^{-1} PTX for 18 h or with 1 μmol·L^{-1} YM 254890 for 30 min and stimulated with 1 μmol·L^{-1} ADPβS (adenosine 5′-[β-thio]diphosphate), 100 μmol·L^{-1} ATPγS (adenosine 5′-[γ-thio] triphosphate), 0.1 μmol·L^{-1} 2-MeSADP [2(methylthio) adenosine 5′-diphosphate], 1 μmol·L^{-1} 2-MeSATP [2(methylthio) adenosine triphosphate], 100 μmol·L^{-1} UDP and 100 μmol·L^{-1} UTP for 30 min. Data are expressed as the percentage of the basal IP level (100%) and represent the mean ± SE of four to seven independent experiments each performed in duplicate. $^{**}P < 0.01$, $^{***}P < 0.001$; a versus basal, b versus agonist response.

not shown) or modify the response of 2-MeSATP (data not shown), which as previously mentioned does not stimulate or inhibit cAMP accumulation in myofibroblasts. Finally, the $P2Y_{12/13}$ antagonist AR-C69931MX had no effect on ADPβS- or ATPγS-induced cAMP responses (data not shown). Overall these data suggest that the $P2Y_{11}$ subtype is functionally expressed and coupled to $G_{q/11}$ in rat myofibroblasts whereas the $P2Y_{13}$ receptor seems not functional, although this subtype is detectable at protein and mRNA levels.

Effect of signalling pathway inhibitors on adenine and uracil nucleotide-induced response in neonatal rat myofibroblasts

The data from the concentration–response curves (Figures 4 and 5) indicate that P2Y receptor subtypes are coupled to $G_{q/11}$ (stimulation of IPs), G_s (increases in cAMP) and G_i proteins (inhibition of forskolin-induced cAMP responses). In order to investigate the role of specific G proteins in P2Y receptor-induced IP and cAMP responses, myofibroblasts were pre-treated with PTX (100 ng·mL^{-1}, 18 h) and YM (1 μmol·L^{-1}, 30 min), specific blockers of G_i and $G_{q/11}$ protein coupling (Takasaki *et al.*, 2004) respectively.

As shown in Figure 8, the $G_{q/11}$ protein inhibitor YM abolished IP responses mediated by, ADPβS, ATPγS, 2-MeSATP, UDP and UTP. It is well known that βγ subunits released following G_i protein activation stimulate PLC and potentiate second messenger responses (IP, Ca^{2+}) mediated by $G_{q/11}$-PCRs (Rebecchi and Pentyala, 2000). In order to investigate a possible interaction between $G_{i/o}$ and $G_{q/11}$, uracil and adenine nucleotides-induced IP accumulation was performed in the presence of PTX (Figure 8). The responses to ADPβS, ATPγS, 2-MeSATP and UTP were insensitive to PTX treatment confirming the involvement of $G_{q/11}$ proteins in IP production. It is notable that IP accumulation mediated by 2-MeSADP was completely blocked by both YM and PTX suggesting that 2-MeSADP stimulates PLC via a positive interaction between both $G_{q/11}$ protein and G_i protein coupling. Interestingly, UDP-induced IP accumulation was significantly enhanced by 58% following PTX treatment indicating that UDP responses involve negative crosstalk between $G_{q/11}$ and G_i protein, which may also explain the biphasic concentration–response curve (Figure 4D). As ADPβS and ATPγS induced cAMP production (Figure 5A), we investigated cAMP accumulation induced by these agonists in the presence or absence of PTX and YM (Figure 9A). No significant effect of PTX and YM on adenine nucleotide-induced cAMP production was observed. However, the inhibition of forskolin-stimulated cAMP accumulation observed with UDP and UTP was completely abolished following PTX pretreatment (Figure 9B). In addition,

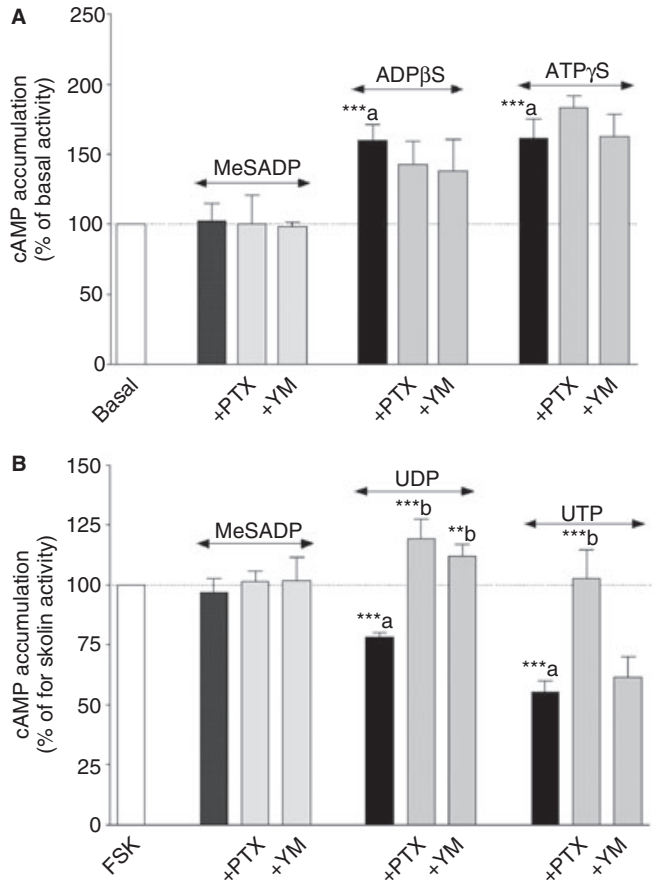

Figure 9 Effect of *Pertussis* toxin (PTX) and YM 254890 (YM) on adenine (panel A) and uracil (panel B) nucleotides-induced cAMP accumulation in neonatal rat cardiac myofibroblasts. Cardiac myofibroblasts were pretreated with 100 ng·mL^{-1} PTX for 18 h or with 1 μmol·L^{-1} YM 254890 for 30 min and stimulated with 100 μmol·L^{-1} ADPβS (adenosine 5′-[β-thio]diphosphate) and 100 μmol·L^{-1} ATPγS (adenosine 5′-[γ-thio] triphosphate) for 15 min (Panel A). Cardiac myofibroblasts were pretreated with 100 ng·mL^{-1} PTX for 18 h or with 1 μmol·L^{-1} YM 254890 for 30 min and stimulated with 100 μmol·L^{-1} UDP and 100 μmol·L^{-1} UTP for 5 min prior to addition of 1.5 μmol·L^{-1} forskolin (FSK) for 10 min (Panel B). Data are expressed as the percentage of the basal cAMP response for adenine nucleotides or forskolin response in the presence of uracil nucleotides (100%) and represent the mean ± SE of four to seven independent experiments each performed in duplicate. $^{**}P < 0.01$, $^{***}P < 0.001$; a versus basal response or forskolin activity, b versus agonist response.

UDP-inhibited forskolin response was also counteracted by YM indicating again a crosstalk between $G_{q/11}$ and $G_{i/o}$ proteins. Finally, the $G_{q/11}$ inhibitor had no effect on UTP-induced inhibition of forskolin response.

Discussion

The purpose of this study was to identify the phenotype of the neonatal rat non-cardiomyocytes used in the study and to characterize the different P2Y receptor subtypes at the expression and functional level in these cells. This report has shown that cardiac myofibroblasts express six P2Y receptor subtypes ($P2Y_{1,2,4,6,11,13}$); however, only five ($P2Y_{1,2,4,6,11}$) were functionally detected.

As mentioned in the *Introduction*, fibroblasts contribute to myocardial function and structure by secreting growth factors, cytokines and components of the ECM such as collagen and fibronectin (Brown *et al.*, 2005; Camelliti *et al.*, 2005). In addition, fibroblasts play an important role in cardiovascular disease. Indeed, the development of fibrosis leading to cardiac dysfunction is the consequence of fibroblast proliferation and their differentiation into myofibroblasts (Wang *et al.*, 2003; Brown *et al.*, 2005). Myofibroblasts express a high level of ECM proteins and generate an abnormal accumulation of ECM, progressing to fibrosis (Brown *et al.*, 2005; Poobalarahi *et al.*, 2006). In addition, myofibroblasts acquire contractile properties by expressing myofilament proteins such as α-smooth muscle actin and vimentin (Wang *et al.*, 2003; Squires *et al.*, 2005; Poobalarahi *et al.*, 2006). Therefore, it was important to determine the phenotype of the cells used in our study given the role of myofibroblasts in cardiac disease. We investigated the expression of the specific marker for cardiac fibroblasts, DDR2, and desmin specifically expressed in smooth and cardiac muscles, and α-smooth muscle actin in the non-cardiomyocytes from our cell culture (Paulin and Li, 2003; Goldsmith *et al.*, 2004). The cells were positive for DDR2 and α-actin, and negative for desmin (Figure 1) as previously reported in differentiated fibroblasts in physiological conditions and in culture (Wang *et al.*, 2003; Squires *et al.*, 2005; Poobalarahi *et al.*, 2006). Myofibroblast differentiation *in vivo* and *in vitro* is produced by several mechanisms including exposure to cytokines, growth factors and ECM components (Wang *et al.*, 2003; Brown *et al.*, 2005; Camelliti *et al.*, 2005). However, the differentiation process of fibroblasts in culture also depends on the culture conditions including serum, support and cell density (Wang *et al.*, 2003; Camelliti *et al.*, 2005). It is noteworthy, and in accordance with our study, that the differentiation of neonatal rat cardiac fibroblasts into myofibroblasts was observed following 2 days in culture and increased from passage 1 to passage 3 over 95% (Wang *et al.*, 2003; Teunissen *et al.*, 2007). These data indicate that previous studies on cardiac fibroblasts were more likely performed on cardiac myofibroblasts or a mixture of fibroblasts and myofibroblasts.

The nucleotides ATP, UTP or both are released during myocardial infarction in human and porcine heart following cardiac ischaemia as well as from cardiomyocytes and pulmonary fibroblasts exposed to ischaemia (Gerasimovskaya *et al.*, 2002; Dutta *et al.*, 2004; Erlinge *et al.*, 2005; Wihlborg *et al.*, 2006). Furthermore, ATP, ADP and UTP generated intracellular Ca^{2+} transients through P2Y receptor stimulation in guinea pig suburothelial myofibroblasts (Wu *et al.*, 2004). Similarly, Liang *et al.* (2008) reported that $P2Y_2$ receptor stimulation by ATP and UTP induced endoplasmic reticulum Ca^{2+} release and Ca^{2+} influx in human valvular myofibroblasts. In our study, all the P2Y agonists induced IP accumulation through $G_{q/11}$ coupling as the $G_{q/11}$ inhibitor YM inhibited all functional response in cardiac myofibroblasts (Figures 4 and 8; Table 3). Adenine nucleotides are preferential agonists for $P2Y_1$, $P2Y_{11}$, $P2Y_{12}$ and $P2Y_{13}$ receptors (Abbracchio *et al.*, 2006; Von Kügelgen, 2006). $P2Y_1$, $P2Y_{11}$ and $P2Y_{13}$ were detected at mRNA and/or protein levels in myofibroblasts (Figures 3 and 4). Although the absence of staining with the peptide antigen indicates that the antibodies recognize their specific target, we

cannot exclude cross reactivity of the anti-$P2Y_1$ and $P2Y_{11}$ antibodies with nuclear proteins, on the basis of propidium iodide and FITC immunofluorescence colocalization inside the nucleus (Figure 3A and I). The functional expression of $P2Y_1$ was confirmed by the effect of the $P2Y_1$ selective antagonist MRS 2179, which partially blocked 2-MeSADP-, ADPβS- (by ≈40%) and ATPγS-induced (by 20%) IP accumulation (Figure 6A and B; Table 4). Interestingly, the $P2Y_{11}$ selective antagonist NF 157 prevented ADPβS-mediated IP production by ≈60% without any effect on the response to ATPγS (Figure 7). These data indicate that the functional response produced by ADPβS is mainly triggered by $P2Y_1$-and $P2Y_{11}$-like receptors in rat myofibroblasts. In addition, ADPβS-mediated IP and cAMP accumulation was not sensitive to PTX (Figures 8A and 9A) indicating that the response to ADPβS was not G_i protein-linked, excluding the involvement of $P2Y_{13}$. Indeed, ADPβS and 2-MeSADP but not the triphosphate nucleotides are potent agonists for the human and rodent $G_{i/o}$ and $G_{q/11}$ proteins-coupled $P2Y_{13}$ receptor (Marteau *et al.*, 2003; Fumagalli *et al.*, 2004). In our study, the $P2Y_{12/13}$ receptor antagonist AR-C69931MX did not affect ADPβS-induced cAMP accumulation (data not shown). Although $P2Y_{13}$ receptor mRNA and protein were detected in our study (Figures 2 and 3K) and PTX partially inhibited 2-MeSADP-induced IP accumulation (Figure 8A), 2-MeSADP had no significant effect on forskolin-stimulated cAMP accumulation (data not shown) and was not modified by PTX treatment (Figure 9B), confirming the lack of $P2Y_{13}$ functional activity in cardiac myofibroblasts. 2-MeSADP-induced IP accumulation was counteracted by the $P2Y_1$ inhibitor (Figure 6A) indicating the involvement of $P2Y_1$ receptor in 2-MeSADP response. In addition, Yoshioka *et al.* (2001) reported that this P2Y subtype forms a heterodimer with the G_i-coupled A_1 adenosine receptor leading to PTX-sensitive responses to ADPβS in co-transfected HEK293T cells. Cardiac fibroblasts express both A_1 and A_{2B} receptors, which inhibit and stimulate cAMP accumulation respectively (Grden *et al.*, 2006). Therefore, we can postulate that the PTX-sensitive response to 2-MeSADP may reflect an interaction with A_1 adenosine receptor rather than a direct activation of a G_i-coupled P2Y receptor, especially as no cAMP response–inhibition and no PTX effect were observed with this agonist. MRS 2179 had no effect on cAMP responses induced by ADPβS and ATPγS (data not shown) indicating that the $P2Y_1$ receptor mediates response through only $G_{q/11}$ coupling as previously reported (Abbracchio *et al.*, 2006; Von Kügelgen, 2006). Similarly, NF 157 had no effect on the cAMP response induced by ADPβS suggesting that the rat $P2Y_{11}$-like receptor is not coupled to G_s protein in myofibroblasts (data not shown). However, the canine and human $P2Y_{11}$ receptors as well as the mouse $P2Y_{11}$-like receptor in adult cardiomyocytes display dual coupling to both $G_{q/11}$ and G_s proteins (Communi *et al.*, 1999; Qi *et al.*, 2001; Balogh *et al.*, 2005). It is noteworthy that ATP, ATPγS and ADPβS induced PTX and YM-insensitive, increases in cAMP accumulation (Figures 4A and 5A, data not shown). The rank order of agonist potency in cAMP accumulation was ATPγS ≈ ADPβS > ATP (Figure 5A; Table 3), which is comparable to the rank order observed for the human $P2Y_{11}$ receptor in transfected cells (Qi *et al.*, 2001). The lack of effect of NF 157 may be a consequence of $P2Y_1$/$P2Y_{11}$ heterodimerization, which appears to modify NF 157 pharmacology (Ecke *et al.*, 2008). Finally, it is possible that adenine nucleotide (including AMP)-mediated increases in cAMP involve a novel P2Y receptor subtype. Overall, these data indicate that the $P2Y_1$ and $P2Y_{11}$ receptors are functionally expressed and coupled to $G_{q/11}$ protein whereas the $P2Y_{13}$ subtype is not functionally expressed.

Uracil nucleotides preferentially activate $P2Y_2$, $P2Y_4$ and $P2Y_6$ receptors (Abbracchio *et al.*, 2006; Von Kügelgen, 2006). RT-PCR and immunocytochemistry confirmed the expression of $P2Y_{2,4,6}$ receptors in neonatal rat cardiac myofibroblasts (Figures 2 and 3). $P2Y_2$ and $P2Y_4$ subtypes are coupled to both $G_{q/11}$ and $G_{i/o}$ proteins whereas the $P2Y_6$ receptor is only coupled to $G_{q/11}$ (Von Kügelgen, 2006; Abbracchio *et al.*, 2006). The selective $P2Y_{2,4,6}$ agonists UTP and UDP induced IP accumulation (Figure 4D) and inhibited forskolin-mediated cAMP production (Figure 5B), which were abolished by YM (Figure 8B) and PTX (Figure 9B) respectively. Therefore, both uracil nucleotides mediated their function through $G_{q/11}$ and $G_{i/o}$ proteins suggesting the functional expression of $P2Y_2$, $P2Y_4$ receptors in neonatal cardiac myofibroblasts. Interestingly, UDP displayed a biphasic IP response, which was potentiated in the presence of PTX suggesting an inhibitory effect on IP production ($G_{q/11}$) via $G_{i/o}$ protein (Figures 4D and 8B) as reported with the opioid κ agonist U-50488H (Misawa *et al.*, 1995). Similarly, the inhibition of forskolin response by UDP was also abolished by YM (Figure 9B) showing an interaction between $G_{q/11}$ and $G_{i/o}$ proteins in UDP-mediated inhibition of cAMP accumulation. Overall, responses to UDP (cAMP, IP) suggest a synergistic interaction between $G_{q/11}$- and $G_{i/o}$-coupled P2Y receptor(s), which may involve $P2Y_2$ and $P2Y_4$ receptor dimers. It is noteworthy that the $P2Y_4$ forms homodimers, and more recently computer modelling suggests that $P2Y_2$ and $P2Y_4$ receptors form heterodimers that exhibit novel pharmacological properties (D'Ambrosi *et al.*, 2006; Fedorov *et al.*, 2007). The functional expression of the $P2Y_6$ receptor and its restricted coupling to $G_{q/11}$ were strengthened by using the selective antagonist MRS 2578, which had no effect on uracil nucleotide-induced inhibition of cAMP response (data not shown) but inhibited IP production mediated by theses agonists (Figure 6D).

In conclusion, although the presence of several P2Y receptor subtypes was a major limitation of this study, we provide for the first time the evidence of the co-expression of five subtypes of P2Y receptor ($P2Y_1$-, $P2Y_2$-, $P2Y_4$-, $P2Y_6$- and $P2Y_{11}$-like) at genomic, protein and functional levels in neonatal rat cardiac myofibroblasts. $P2Y_1$-, $P2Y_2$-, $P2Y_4$-, $P2Y_6$- and $P2Y_{11}$-like receptors primarily mediate their function through $G_{q/11}$ protein coupling. In addition, $P2Y_{2,4}$ subtypes are also coupled to $G_{i/o}$. Although $P2Y_{13}$ receptor mRNA and protein were detected, no evidence was shown regarding the functional activity of this subtype. Finally, independent of a coupling to G_i and G_q proteins, the G_s response induced by the adenine nucleotides suggests the expression of a new P2Y receptor subtype. The expression of different P2Y subtypes stimulated by multiple endogenous agonists suggests a complex physiological role of nucleotide receptors in regulating cardiac myofibroblast function, particularly in heart disease where these cells mediate fibrosis, and adenine as well as uracil nucleotides are released.

Acknowledgements

This work was supported by Nottingham Trent University. We are grateful to Dr M Taniguchi (Yamanouchi Pharmaceutical Co., Ltd., Ibaraki, Japan) and Astra Zeneca for kindly providing YM and AR-C69931MX respectively.

Conflict of interest

The authors state no conflict of interest.

References

Abbracchio MP, Burnstock G, Boeynaems J-M, Barnard EA, Boyer JL, Kennedy C *et al.* (2006). International union of pharmacology LVIII: update on the P2Y G protein-coupled nucleotide receptors: from molecular mechanisms and pathophysiology to therapy. *Pharmacol Rev* **58**: 281–341.

Alexander SPH, Mathie A, Peters JA (2008). Guide to Receptors and Channels (GRAC), 3rd edn. *Br J Pharmacol* **153** (Suppl. 2): S1–S209.

Balogh J, Wihlborg AK, Isackson H, Joshi BV, Jacobson KA, Erlinge D (2005). Phospholipase C and cAMP-dependent positive inotropic effects of ATP in mouse cardiomyocytes via $P2Y_{11}$-like receptors. *J Mol Cell Cardiol* **39**: 223–230.

Boyer JL, Mohanram A, Camaioni E, Jacobson KA, Harden TK (1998). Competitive and selective antagonism of P2Y1 receptors by N^6-methyl 2′-deoxyadenosine 3′,5′-biphosphate. *Br J Pharmacol* **124**: 1–3.

Brown RD, Ambler SK, Mitchell MD, Long CS (2005). The cardiac fibroblast: therapeutic target in myocardial remodelling and failure. *Annu Rev Pharmacol Toxicol* **45**: 657–688.

Brown SG, King BF, Kim Y, Jang SY, Burnstock G, Jacobson KA (2000). Activity of novel adenine nucleotide derivatives as agonists and antagonists at recombinant rat P2X receptors. *Drug Develop Res* **49**: 253–259.

Camelliti P, Borg TK, Kohl P (2005). Structural and functional characterisation of cardiac fibroblast. *Cardiovasc Res* **65**: 40–51.

Chootip K, Gurney AM, Kennedy C (2005). Multiple P2Y receptors couple to calcium-dependent, chloride channels in smooth muscle cells of the rat pulmonary artery. *Respir Res*: 124–133.

Communi D, Robaye B, Boeynaems J-M (1999). Pharmacological characterization of the human $P2Y_{11}$ receptor. *Br J Pharmacol* **128**: 1199–1206.

D'Ambrosi N, Iafrate M, Vacca F, Amadio S, Tozzi A, Mercuri NB *et al.* (2006). The $P2Y_4$ receptor forms homo-oligomeric complexes in several CNS and PNS neuronal cells. *Purinergic Signalling* **2**: 575–582.

Dickenson JM, Hill SJ (1998). Potentiation of adenosine A1 receptor-mediated inositol phospholipid hydrolysis by tyrosine kinase inhibitors in CHO cells. *Br J Pharmacol* **125**: 1049–1057.

Dubey RK, Gillespie DG, Jackson EK (1998). Adenosine inhibits collagen and protein synthesis in cardiac fibroblasts: role of A_{2B} receptors. *Hypertension* **31**: 943–948.

Dutta AK, Sabirov RZ, Uramoto H, Okada Y (2004). Role of ATP-conductive anion channel in ATP release from neonatal rat cardiomyocytes in ischaemic or hypoxic conditions. *J Physiol* **559**: 799–812.

Ecke D, Hanck T, Tulapurkar ME, Schafer R, Kassack M, Stricker R *et al.* (2008). Hetero-oligomerization of $P2Y_{11}$ receptor with P2Y1 receptor controls the internalization and ligand selectivity of the $P2Y_{11}$ receptor. *Biochem J* **409**: 107–116.

Erlinge D, Harnek J, van Heusden C, Olivecrona G, Jern S, Lazarowski E (2005). Uridine triphosphate (UTP) is released during cardiac ischemia. *Int J Cardiol* **100**: 427–433.

Fedorov IV, Rogachevskaja OA, Kolesnikov SS (2007). Modeling P2Y receptor-Ca^{2+} response coupling in taste cells. *Biochim Biophys Acta* **1768**: 1727–1740.

Fredholm BB, Ijzerman AP, Jacobson KA, Klotz K-N, Linden J (2001). International Union of Pharmacology. XXV. Nomenclature and classification of adenosine receptors. *Pharmacol Rev* **53**: 527–552.

Froldi G, Varani K, Chinellato A, Ragazzi E, Caparrotta L, Borea PA (1997). P2X-purinoceptors in the heart: actions of ATP and UTP. *Life Sci* **60**: 1419–1430.

Fumagalli M, Trincavelli L, Lecca D, Martini C, Ciana P, Abbracchio MP (2004). Cloning, pharmacological characterisation and distribution of the rat G-protein coupled $P2Y_{13}$ receptor. *Biochem Pharmacol* **68**: 113–124.

Gachet C (2005). The platelet P2 receptors as molecular targets for old and new antiplatelet drugs. *Pharmacol Ther* **108**: 180–192.

Gao N, Hu HZ, Liu S, Gao C, Xia Y, Wood JD (2007). Stimulation of adenosine A1 and A2A receptors by AMP in the submucosal plexus of guinea pig small intestine. *Am J Physiol* **292**: 492–500.

Gerasimovskaya EV, Ahmad S, White CW, Jones PL, Carpenter TC, Stenmark KR (2002). Extracellular ATP is an autocrine/paracrine regulator of hypoxia-induced adventitial fibroblast growth. *J Biol Chem* **277**: 44638–44650.

Germack R, Dickenson JM (2006). Induction of β_3-adrenergic receptor functional expression following chronic stimulation with noradrenaline in neonatal rat cardiomyocytes. *J Pharmacol Exp Ther* **316**: 392–402.

Goldsmith EC, Hoffman A, Morales MO, Potts JD, Price RL, McFadden A *et al.* (2004). Organization of fibroblasts in the heart. *Developmental Dynamics* **230**: 787–794.

Grden M, Podgorska M, Kocbuch K, Szutowicz A, Pawelczyk T (2006). Expression of adenosine receptors in cardiac fibroblasts as a function of insulin and glucose level. *Arch Biochem Biophys* **455**: 10–17.

Hansen MA, Bennett MR, Barden JA (1999). Distribution of purinergic P2X receptors in the rat heart. *J Auton Nerv Syst* **78**: 1–9.

Hou M, Malmsjo M, Moller S, Pantev E, Bergdahl A, Zhao XH *et al.* (1999). Increase in cardiac P2X1-and P2Y2-receptor mRNA levels in congestive heart failure. *Life Sci* **65**: 1195–1206.

Lakshmi S, Joshi PG (2006). Activation of Src/kinase/phospholipase C/mitogen-activated protein kinase and induction of neurite expression by ATP, independent of nerve growth factor. *Neuroscience* **141**: 179–189.

Lee SC, Vielhauer NS, Leaver EV, Pappone PA (2005). Differential regulation of Ca^{2+} signaling and membrane trafficking by multiple P2 receptors in brown adipocytes. *J Membr Biol* **207**: 131–142.

Liang W, McDonald P, McManus B, Van Breemen C, Wang X (2008). P2Y2 receptor-mediated Ca^{2+} signalling and spontaneous Ca^{2+} releases in human vavular myofibroblasts. *Int Heart J* **49**: 221–236.

Mamedova LK, Joshi BV, Gao ZG, von Kugelgen I, Jacobson KA (2004). Diisothiocyanate derivatives as potent, insurmountable antagonists of P2Y6 nucleotide receptors. *Biochem Pharmacol* **67**: 1763–1770.

Marteau F, Le Poul E, Communi D, Communi D, Labouret C, Savi P *et al.* (2003). Pharmacological characterization of the human $P2Y_{13}$ receptor. *Mol Pharmacol* **64**: 104–112.

Meszaros JG, Gonzalez AM, Endo-Mochizuki Y, Villegas S, Villarreal F, Brunton LL (2000). Identification of G protein-coupled signalling pathways in cardiac fibroblasts: cross talk between Gq/11 and Gs. *Am J Physiol* **278**: C154–C162.

Misawa H, Ueda H, Katada T, Ui M, Satoh M (1995). A subtype of opioid κ-receptor is coupled to inhibition of Gi1-mediated phospholipase C activity in the guinea pig cerebellum. *FEBS Lett* **361**: 106–110.

Moore GJ, Scanlon MN (1989). Methods for analyzing and interpreting cooperativity in dose-response curves-I. Antagonist effects on angiotensin receptors in smooth muscle. *Gen Pharmacol* **20**: 193–198.

Paulin D, Li Z (2003). Desmin: a major intermediate filament protein

essential for the structural integrity and function of muscle. *Exp Cell Res* **301**: 1–7.

Poobalarahi F, Baicu CF, Bradshaw AD (2006). Cardiac myofibroblasts differentiated in 3D culture exhibit distinct changes in collagen I production, processing, and matrix deposition. *Am J Physiol* **291**: H2924–H2932.

Qi A-D, Zambon AC, Insel PA, Nicholas RA (2001). An arginine/glutamine difference at the juxtaposition of ransmembrane domain 6 and third extracellular loop contributes to the markedly different nucleotide selectivities of human and canine $P2Y_{11}$ receptors. *Mol Pharmacol* **60**: 1375–1382.

Rebecchi MJ, Pentyala SN (2000). Structure, function, and control of phosphoinositide-specific phospholipase C. *Physiol Rev* **80**: 1291–1335.

Sak K, Webb TE (2002). A retrospective of recombinant P2Y receptor subtypes and their pharmacology. *Arch Biochem Biophys* **397**: 131–136.

Scrivens M, Dickenson JM (2005). Functional expression of the $P2Y_{14}$ receptor in murine T-lymphocytes. *Br J Pharmacol* **146**: 435–444.

Squires CE, Escobar GP, Payne JF, Leonardi RA, Goshorn DK, Sheats NJ *et al*. (2005). Altered fibroblast function following myocardial infarction. *J Mol Cell Cardiol* **39**: 699–707.

Takasaki J, Saito T, Taniguchi M, Kawasaki T, Moritani Y, Hayashi K *et al*. (2004). A novel $G\alpha_{q/11}$-selective inhibitor. *J Biol Chem* **279**: 47438–47445.

Teunissen BEJ, Smeets PJH, Willemsen PHM, De Windt LJ, Van der Vusse GJ, Van Bilsen M (2007). Activation of PPARδ inhibits cardiac fibroblasts proliferation and the transdifferentiation into myofibroblasts. *Cardiovasc Res* **75**: 519–529.

Ullmann H, Meis S, Hongwiset D, Marzian C, Wiese M, Nickel P *et al*. (2005). Synthesis and structure-activity relationships of suramin-derived $P2Y_{11}$ receptor antagonists with nanomolar potency. *J Med Chem* **48**: 7040–7048.

Von Kügelgen I (2006). Pharmacological profiles of cloned mammalian P2Y-receptor subtypes. *Pharmacol Ther* **110**: 415–432.

Wang J, Chen H, Seth A, McCulloch CA (2003). Mechanical force regulation of myofifroblast differentiation in cardiac fibroblasts. *Am J Physiol* **285**: H1871–H1881.

Webb TE, Boluyt MO, Barnard EA (1996). Molecular biology of P2Y purinoceptors: expression in rat heart. *J Auton Pharmacol* **16**: 303–307.

Wihlborg AK, Balogh J, Wang L, Borna C, Dou Y, Joshi BV *et al*. (2006). Positive inotropic effects by uridine triphosphate (UTP) and uridine diphosphate (UDP) via P2Y2 and P2Y6 receptors on cardiomyocytes and release of UTP in man during myocardial infarction. *Circ Res* **98**: 970–976.

Wu C, Sui GP, Fry CH (2004). Purinergic regulation of guinea pig suburothelial myofibroblasts. *J Physiol* **559**: 231–243.

Yitzhaki S, Shainberg A, Cheporko Y, Vidne BA, Sagie A, Jacobson KA *et al*. (2006). Uridine-5-triphosphate (UTP) reduces infarct size and improves rat heart function after myocardial infarct. *Biochem Pharmacol* **72**: 949–955.

Yoshioka K, Saitoh O, Nakata H (2001). Heteromeric association creates a P2Y-like adenosine receptor. *Proc Natl Acad Sci* **98**: 7617–7622.

Zhang FL, Luo L, Gustafson E, Palmer K, Qiao X, Fan X *et al*. (2002). $P2Y_{13}$: identification and characterization of a novel Gai-coupled ADP receptor from human and Mouse. *J Pharmacol Exp Ther* **301**: 705–713.

Zheng JS, O'Neill L, Long X, Webb TE, Barnard EA, Lakatta EG *et al*. (1998). Stimulation of P2Y receptors activates *c-fos* gene expression and inhibits DNA synthesis in cultured cardiac fibroblasts. *Cardiovasc Res* **37**: 718–728.